26th ABCM International Congress of Mechanical Engineering
November 22-26, 2021. Florianópolis, SC, Brazil

COB-2021-0702
DISTURBANCE OBSERVER OF AN UAV WITH A SUSPENDED PAYLOAD

Renan Cavenaghi Silva[1]
Douglas Domingues Bueno[2]
São Paulo State University (UNESP), School of Engineering of Ilha Solteira, Dept. of Mechanical Engineering[1], Dept. of Mathematics[2], Av. Brasil 56, Ilha Solteira, SP, Brazil
cavenaghi.silva@unesp.br[1]
douglas.bueno@unesp.br[2]

Rodrigo Borges Santos[3]
Grande Dourados Federal University (UFGD), Dept. of Mechanical Engineering[3], R. João Rosa Góes 1761, Dourados - MS, Brazil
rodrigobsantos@ufgd.edu.br[3]

Abstract. *Applications that are being envisioned to be realized by Unmanned Aerial Vehicles (UAV) have a common requisite of transporting payloads to diverse locations, which can be done by suspending the payload with cables. However, the UAV control uses a simplified dynamical model in which disturbances resulting from non-modeled dynamics and the environment may degrade system performance. One strategy to deal with disturbances is the Disturbance Observer Based Control, which uses a disturbance observer to estimate the disturbance and calculate adequate control terms to reduce the effect of the disturbance on the system. To implement this strategy to the transport of suspended payload with and UAV, the nonlinear dynamical model of an UAV with a suspended payload is obtained using the Euler-Lagrange formalism. A disturbance observer using the linearized dynamics is designed to estimate the disturbance forces and use in the controller loop to track mission trajectories. The nonlinear model is simulated using the fifth-order Runge-Kutta algorithm and the results demonstrated the effectiveness of the disturbance observer to obtain estimates for the disturbances forces resulting from wind drag; furthermore, using the disturbance observer an improvement in the tracking control performance is indicated using performance metrics.*

Keywords: *Unmanned Aerial Vehicles, Control, Observer, Simulation.*

1. INTRODUCTION

Unmanned Aerial Vehicles (UAV) have been used for many applications that are dangerous to be realized by manned vehicles. They can be employed for autonomous operations and involve low costs in comparison with manned aircraft. UAV can be used to transport different types of payloads, such as food, medical supplies, electronic devices, and others, attracting interest from delivery companies mainly due to the advantages in logistics that can be achieved by a fleet of autonomous vehicles in comparison with other conventional procedures. However, the UAV controller normally use a nominal plant for reference and effects like blade flapping, propeller gyroscopic torques, model uncertainties and external sources like wind gusts can affect the UAV motion. In the perspective of the controller, these effects can be lumped as disturbances forces acting on the UAV dynamical model and it is of interest to reduce these effects by using an observer to calculate estimatives of the disturbance forces.

Disturbances are unavoidable in real world applications and result in adverse effects in the controller performance, with potential to destabilize the system depending on the magnitude (Xie and Guo, 2000). Forces like wind gusts and friction can be treated as external disturbances and model uncertainties or unmodeled dynamics treated as internal disturbances (Chen *et al.*, 2016). Generally, these disturbances are difficult or impractical to measure; but, in the Disturbance Observer Based Control (DOBC) framework, a Disturbance Observer (DO) is used to calculate estimates of the disturbances forces using identified dynamics and measurable states (Sariyildiz *et al.*, 2020). Based on the disturbance estimate, it is possible to calculate control inputs to compensate for the influence of the disturbance, increasing the mission performance. This strategy is successfully applied in applications like precision positioning of robots (Chen and Cheng, 2012) and suppressing suspended payload oscillation in overhead cranes (Niu *et al.*, 2020).

In the aerial transportation of payloads, the UAV act as a flying crane transporting the payload to the desired trajectories. The UAV and suspended payload system have coupled dynamics and effects applied to the payload are transmitted to the UAV, resulting in a negative effect to the control performance. Additionally, since an UAV normally uses the plant of a system composed only by the UAV, the forces resulting from the payload dynamics are not considered and can be

treated as disturbances forces.

The remaining of this work is divided in four parts: in Section 2 is the description of the problem, mathematical modeling and design of the disturbance observer. Section 3 presents the controller to stabilize the system and track desired trajectories. Section 4 presents the simulations results and their discussion. Finally in Section 5 are the conclusions.

2. DYNAMIC MODEL

The object of study consist of a class of multirotor UAV characterized by multiple propellers distributed in the structure. The mission is represented in Fig. 1 and consist of moving the UAV by a desired trajectory ${}_{\mathcal{I}}\mathbf{r}_d = \begin{Bmatrix} x_d & y_d & z_d \end{Bmatrix}^T$, represented by the dashed cyan lines. To model the dynamics of this system, two coordinated frames are defined, an inertial coordinate frame $\mathcal{I} : \left\{O, \hat{i}, \hat{j}, \hat{z}\right\}$ and the body coordinate frame $\mathcal{B} : \left\{O', {}_{\mathcal{B}}\hat{i}, {}_{\mathcal{B}}\hat{j}, {}_{\mathcal{B}}\hat{k}\right\}$ aligned with the principal inertia axis and fixed to the UAV center of mass O' positioned at ${}_{\mathcal{I}}\mathbf{r} = \begin{Bmatrix} x & y & z \end{Bmatrix}^T$ in the inertial frame of reference. The UAV has mass m and a payload of mass m_p suspended using a massless rigid rod of length l attached to the UAV center of mass. The UAV and payload are subjected to an external disturbance force ${}_{\mathcal{I}}\mathbf{d} = \begin{Bmatrix} {}_{\mathcal{I}}\mathbf{d}_v & {}_{\mathcal{I}}\mathbf{d}_p \end{Bmatrix}^T$ represented in the figure by arrows colored in magenta.

Notation: for the remaining of this work, $\mathbf{A}^T$ indicates the transpose of $\mathbf{A}$. s_x and c_x indicates $\sin x$ and $\cos x$ respectively. The left subscript indicate the frame of reference of the corresponding vector.

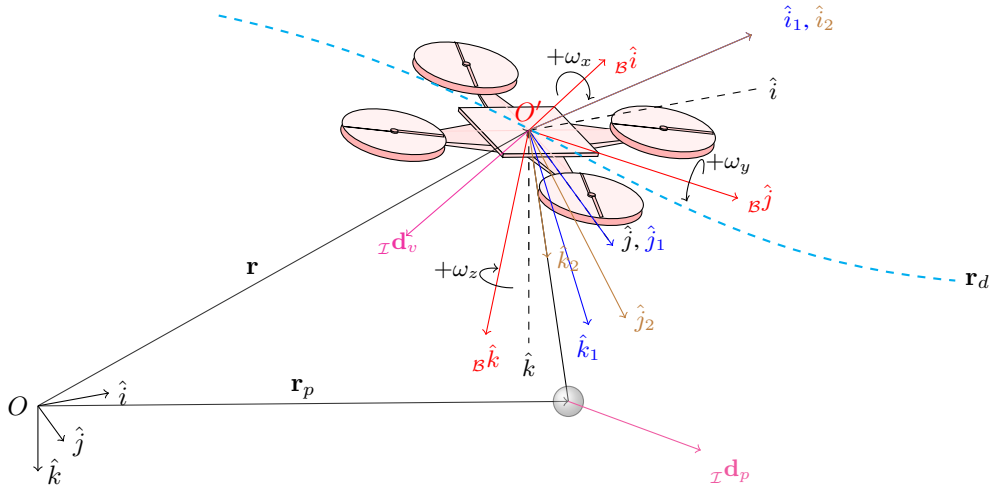

Figure 1: UAV with suspended payload.

2.1 Equations of Motion

The Euler angles representation are utilized to parameterize the body rotations. To transform a vector from the inertial frame to the body frame of reference three consecutive transformation are performed: a yaw rotation defined by transformation $\psi : (\hat{i},\ \hat{j},\ \hat{k}) \xrightarrow{\mathbf{T}_\psi} (\hat{i}',\ \hat{j}',\ \hat{k}')$, a pitch rotation $\theta : (\hat{i}',\ \hat{j}',\ \hat{k}') \xrightarrow{\mathbf{T}_\theta} (\hat{i}'',\ \hat{j}'',\ \hat{k}'')$ and the roll rotation $\phi : (\hat{i}'',\ \hat{j}'',\ \hat{k}'') \xrightarrow{\mathbf{T}_\phi} ({}_{\mathcal{B}}\hat{i},\ {}_{\mathcal{B}}\hat{j},\ {}_{\mathcal{B}}\hat{k})$. The sequence of transformations are indicated in Eq. 1:

$$\begin{aligned} {}_{\mathcal{B}}\mathbf{r} &= \underbrace{\mathbf{T}_\phi \mathbf{T}_\theta \mathbf{T}_\psi}_{\mathbf{R}} {}_{\mathcal{I}}\mathbf{r} \\ &= \mathbf{R}\, {}_{\mathcal{I}}\mathbf{r} \end{aligned} \tag{1}$$

where $\mathbf{R}$ is the rotation matrix and the rotation matrices are defined as:

$$\mathbf{R} = \begin{bmatrix} c_\theta c_\psi & s_\psi c_\theta & -s_\theta \\ s_\phi s_\theta c_\psi - s_\psi c_\phi & s_\phi s_\theta s_\psi + c_\phi c_\psi & s_\phi c_\theta \\ c_\phi s_\theta c_\psi + s_\phi s_\psi & c_\phi s_\theta s_\psi - s_\phi c_\psi & c_\phi c_\theta \end{bmatrix}, \tag{2}$$

$$\mathbf{T}_\psi = \begin{bmatrix} c_\psi & s_\psi & 0 \\ -s_\psi & c_\psi & 0 \\ 0 & 0 & 1 \end{bmatrix},$$

$$\mathbf{T}_\theta = \begin{bmatrix} c_\theta & 0 & -s_\theta \\ 0 & 1 & 0 \\ s_\theta & 0 & c_\theta \end{bmatrix},$$

$$\mathbf{T}_\phi = \begin{bmatrix} 1 & 0 & 0 \\ 0 & c_\phi & s_\phi \\ 0 & -s_\phi & c_\phi \end{bmatrix}.$$

2.1.1 Payload Position

The payload is parameterized as function of two rotations, a first rotation $\beta : (\hat{i}, \hat{j}, \hat{k}) \xrightarrow{\mathbf{T}_\beta} (\hat{i}_1,\ \hat{j}_1,\ , \hat{k}_1)$ in the $\hat{j}$ axis, and a second rotation $\alpha : (\hat{i}_1,\ \hat{j}_1,\ \hat{k}_1) \xrightarrow{\mathbf{T}_\alpha} (\hat{i}_2,\ \hat{j}_2,\ \hat{k}_2)$ about the $\hat{i}_1$ axis. This choice of rotations is performed to avoid singularity in the inertia matrix when the payload is aligned with the positive inertial k direction, which corresponds to a stable equilibrium point in a pendulum system. The payload position in the inertial frame described by the generalized coordinates α and β is:

$$_{\mathcal{I}}\mathbf{r}_p = \begin{Bmatrix} x + lc_\alpha s_\beta \\ y - ls_\alpha \\ z + lc_\alpha c_\beta \end{Bmatrix} \tag{3}$$

2.1.2 UAV Angular Velocity

The angular velocity of the UAV in the body reference frame ${}_{\mathcal{B}}\omega = \{\omega_x,\ \omega_y,\ \omega_z\}^T$ is related to the yaw, pitch and roll angular velocities with the following relation:

$$_{\mathcal{B}}\omega = \mathbf{T}_\phi \mathbf{T}_\theta \mathbf{T}_\psi \begin{Bmatrix} 0 \\ 0 \\ \dot{\psi} \end{Bmatrix} + \mathbf{T}_\phi \mathbf{T}_\theta \begin{Bmatrix} 0 \\ \dot{\theta} \\ 0 \end{Bmatrix} + \mathbf{T}_\phi \begin{Bmatrix} \dot{\phi} \\ 0 \\ 0 \end{Bmatrix} \tag{4}$$

$$= \begin{Bmatrix} -\dot{\psi}s_\theta + \dot{\phi} \\ \dot{\psi}s_\phi c_\theta + \dot{\theta}c_\phi \\ \dot{\psi}c_\phi c_\theta - \dot{\theta}s_\phi \end{Bmatrix} \tag{5}$$

$$= \begin{bmatrix} 1 & 0 & -s_\theta \\ 0 & c_\phi & s_\phi c_\theta \\ 0 & -s_\phi & c_\phi c_\theta \end{bmatrix} \begin{Bmatrix} \dot{\phi} \\ \dot{\theta} \\ \dot{\psi} \end{Bmatrix} \tag{6}$$

2.1.3 Euler-Lagrange Equations

In order to obtain the equations of motion, the kinetic energy is:

$$\mathcal{T} = \frac{1}{2}\, _{\mathcal{I}}\dot{\mathbf{r}}_p^T m_p\, _{\mathcal{I}}\dot{\mathbf{r}}_p + \frac{1}{2}\, _{\mathcal{I}}\dot{\mathbf{r}}^T m\, _{\mathcal{I}}\dot{\mathbf{r}} + \frac{1}{2}\, _{\mathcal{B}}\omega^T \mathbf{J}\, _{\mathcal{B}}\omega \tag{7}$$

with the principal inertia matrix defined as:

$$\mathbf{J} = \begin{bmatrix} I_{xx} & 0 & 0 \\ 0 & I_{yy} & 0 \\ 0 & 0 & I_{zz} \end{bmatrix} \tag{8}$$

The potential energy from the system is the sum of the potential energy of the quadrotor and the suspended payload and is calculated as:

$$\mathcal{U} = -mgz - m_p g\left(z + lc_\alpha c_\beta\right). \tag{9}$$

The Lagrangian, defined as $\mathcal{L} = \mathcal{T} - \mathcal{U}$, is utilized to calculate the equations of motion using the Euler-Lagrange equation, Eq. 10, for each generalized coordinate $q_k \in \{x, y, z, \phi, \theta, \psi, \alpha, \beta\}$:

$$\frac{d}{dt}\left(\frac{\partial \mathcal{L}}{\partial \dot{q}_k}\right) - \frac{d}{dt}\left(\frac{\partial \mathcal{L}}{\partial q_k}\right) = Q_k. \tag{10}$$

2.1.4 Generalized Forces

The forces acting on the system are resulting from the control inputs and disturbances acting on the UAV and payload. The disturbance forces can be incorporated in the equations by calculating:

$$Q_k = \sum_{i=0}^{N_{UAV}} f_i \cdot \frac{\partial\, _{\mathcal{I}}\mathbf{r}}{\partial q_k} + \sum_{i=0}^{N_p} f_i \cdot \frac{\partial\, _{\mathcal{I}}\mathbf{r}_p}{\partial q_k} \tag{11}$$

with i indicating the i-th force

$$Q_x = (c_\phi s_\theta c_\psi + s_\phi s_\psi)\, U_1 + d_{v,\hat{i}} + d_{p,\hat{i}} \tag{12a}$$
$$Q_y = (c_\phi s_\theta s_\psi - s_\phi c_\psi)\, U_1 + d_{v,\hat{j}} + d_{p,\hat{j}} \tag{12b}$$
$$Q_z = (c_\phi c_\theta)\, U_1 + d_{v,\hat{k}} + d_{p,\hat{k}} \tag{12c}$$
$$Q_\phi = U_2 \tag{12d}$$
$$Q_\theta = U_3 \tag{12e}$$
$$Q_\psi = U_4 \tag{12f}$$
$$Q_\alpha = -\, d_{p,\hat{i}} l s_\alpha s_\beta - d_{p,\hat{j}} l c_\alpha - d_{p,\hat{k}} l s_\alpha c_\beta \tag{12g}$$
$$Q_\beta = d_{p,\hat{i}} l c_\alpha c_\beta - d_{p,\hat{k}} l c_\alpha s_\beta \tag{12h}$$

where ${}_{\mathcal{I}}\mathbf{d}_p = \left\{ d_{p,\hat{i}},\ d_{p,\hat{j}},\ d_{p,\hat{k}} \right\}$ and ${}_{\mathcal{I}}\mathbf{d}_v = \left\{ d_{v,\hat{i}},\ d_{v,\hat{j}},\ d_{v,\hat{k}} \right\}$ are the disturbances forces components applied to the UAV and payload; and U_1, U_2, U_3 and U_4 are the abstract control inputs relating the lift and drag from the propellers to the force and moment described in the UAV center of mass.

2.2 System Dynamics

The system of equations obtained using the Euler-Lagrange equations, defined by Eq. 10, can be represented in the form of a system of nonlinear second order differential equations as:

$$\mathbf{M}(\mathbf{q})\ddot{\mathbf{q}} + \mathbf{C}(\mathbf{q}, \dot{\mathbf{q}})\dot{\mathbf{q}} + \mathbf{G}(\mathbf{q}) = \mathbf{B}(\mathbf{q})\mathbf{u} + \mathbf{E}(\mathbf{q})\mathbf{d}, \tag{13}$$

where the matrices are defined as:

$$\mathbf{M}(\mathbf{q}) = \begin{bmatrix} m+m_p & 0 & 0 & 0 & 0 & 0 & -m_p l s_\alpha s_\beta & m_p l c_\alpha c_\beta \\ 0 & m+m_p & 0 & 0 & 0 & 0 & -m_p l c_\alpha & 0 \\ 0 & 0 & m+m_p & 0 & 0 & 0 & -m_p l s_\alpha c_\beta & -m_p l c_\alpha s_\beta \\ 0 & 0 & 0 & I_{xx} & 0 & -I_{xx} s_\theta & 0 & 0 \\ 0 & 0 & 0 & 0 & m_{55} & m_{56} & 0 & 0 \\ 0 & 0 & 0 & -I_{xx} s_\theta & m_{65} & m_{66} & 0 & 0 \\ -m_p l s_\alpha s_\beta & -m_p l c_\alpha & -m_p l s_\alpha c_\beta & 0 & 0 & 0 & m_p l^2 & 0 \\ m_p l c_\alpha c_\beta & 0 & -m_p l s_\beta c_\alpha & 0 & 0 & 0 & 0 & m_p l^2 c_\alpha^2 \end{bmatrix},$$

with $m_{55} = I_{yy} c_\phi^2 + I_{zz} s_\phi^2$, $m_{56} = m_{65} = s_\phi c_\phi c_\theta (I_{yy} - I_{zz})$ e $m_{66} = I_{xx} s_\theta^2 + c_\theta^2 (I_{yy} s_\phi^2 + I_{zz} c_\phi^2)$,

$$\mathbf{C}(\mathbf{q}, \dot{\mathbf{q}}) = \begin{bmatrix} 0 & 0 & 0 & 0 & 0 & 0 & m_p l(-c_\alpha s_\beta \dot{\alpha} - s_\alpha c_\beta \dot{\beta}) & m_p l(-s_\alpha c_\beta \dot{\alpha} - s_\alpha s_\beta \dot{\beta}) \\ 0 & 0 & 0 & 0 & 0 & 0 & m_p l s_\alpha \dot{\alpha} & 0 \\ 0 & 0 & 0 & 0 & 0 & 0 & m_p l \left(-c_\alpha c_\beta \dot{\alpha} + s_\alpha s_\beta \dot{\beta}\right) & m_p l \left(s_\alpha s_\beta \dot{\alpha} - c_\alpha c_\beta \dot{\beta}\right) \\ 0 & 0 & 0 & c_{44} & c_{45} & c_{46} & 0 & 0 \\ 0 & 0 & 0 & c_{54} & c_{55} & c_{56} & 0 & 0 \\ 0 & 0 & 0 & c_{64} & c_{65} & c_{66} & 0 & 0 \\ 0 & 0 & 0 & 0 & 0 & 0 & 0 & m_p l^2 s_\alpha c_\alpha \dot{\beta} \\ 0 & 0 & 0 & 0 & 0 & 0 & -m_p l^2 s_\alpha c_\alpha \dot{\beta} & -m_p l^2 s_\alpha c_\alpha \dot{\alpha} \end{bmatrix}$$

with $c_{45} = s_\phi c_\phi (I_{yy} - I_{zz})\dot{\theta} + s_\phi^2 c_\theta (I_{yy} - I_{zz})\dot{\psi}$, $c_{46} = s_\phi c_\phi c_\theta^2 (I_{zz} - I_{yy})\dot{\psi} + c_\phi^2 c_\theta (I_{zz} - I_{yy})\dot{\theta} - I_{xx} c_\theta \dot{\theta}$, $c_{54} = I_{zz}\dot{\psi} c_\theta + (I_{yy} - I_{xx})(-\dot{\theta} s_\theta c_\phi + \dot{\psi} c_\theta c_\phi^2 - \dot{\psi} c_\theta s_\phi^2)$, $c_{55} = -(I_{yy} - I_{xx}) s_\phi c_\phi \dot{\phi}$, $c_{56} = \dot{\psi} s_\theta c_\theta (-I_{zz} + I_{yy} s_\phi^2 + I_{xx} c_\phi^2)$, $c_{64} = -(I_{xx}\dot{\theta} c_\theta - (I_{yy} - I_{xx})(\dot{\psi} c_\theta^2 s_\phi c_\phi))$, $c_{65} = I_{zz}\dot{\psi} s_\theta c_\theta - (I_{yy} - I_{xx})(\dot{\theta} s_\theta c_\phi s_\phi + \dot{\phi} c_\theta s_\phi^2) - (I_{yy} + I_{xx})(\dot{\psi} s_\theta c_\theta c_\phi^2 - \dot{\phi} c_\theta c_\phi^2)$, $c_{66} = I_{zz}\dot{\theta} s_\theta c_\theta - (I_{yy} + I_{xx})(\dot{\theta} s_\theta c_\theta s_\phi^2) + (I_{yy} - I_{xx})\dot{\phi} c_\theta^2 s_\phi c_\phi$,

$$\mathbf{G}(\mathbf{q}) = \begin{bmatrix} \mathbf{0}_{2\times 1} \\ -(m+m_p)g \\ \mathbf{0}_{3\times 1} \\ m_p g l s_\alpha c_\beta \\ m_p g l c_\alpha s_\beta \end{bmatrix},$$

$$\mathbf{B}(\mathbf{q}) = \begin{bmatrix} c_\phi s_\theta c_\psi + s_\phi s_\psi & \mathbf{0}_{1\times 3} \\ c_\phi s_\theta s_\psi - s_\phi c_\psi & \mathbf{0}_{1\times 3} \\ c_\phi c_\theta & \mathbf{0}_{1\times 3} \\ \mathbf{0}_{3\times 1} & \mathbf{I}_{3\times 3} \\ \mathbf{0}_{2\times 1} & \mathbf{0}_{2\times 3} \end{bmatrix},$$

and the control vector defined as:

$$\mathbf{u} = \begin{Bmatrix} U_1 & U_2 & U_3 & U_4 \end{Bmatrix}^T.$$

The disturbance matrix is:

$$\mathbf{E}(\mathbf{q}) = \begin{bmatrix} \mathbf{I}_{3\times3} & & \mathbf{I}_{3\times3} & \\ \mathbf{0}_{3\times3} & & \mathbf{0}_{3\times3} & \\ \mathbf{0}_{1\times3} & -ls_\alpha s_\beta & -lc_\alpha & -ls_\alpha c_\beta \\ \mathbf{0}_{1\times3} & lc_\alpha c_\beta & 0 & lc_\alpha s_\beta \end{bmatrix}.$$

2.2.1 System Equations

The Euler-Lagrange equations obtained in Eq.10 results in a system of n differential equations of second order, with n equals to the number of generalized coordinates. To solve the equations for $\mathbf{q}$ using a numerical method, like the family of Runge-Kutta methods, a variable substitution $v_k = \dot{q}_k$ is realized to obtain a system of $2n$ differential equations of first order. This substitution results in the following system:

$$\begin{Bmatrix} \dot{\mathbf{q}} \\ \dot{\mathbf{v}} \end{Bmatrix} = \begin{bmatrix} \mathbf{0} & \mathbf{I} \\ \mathbf{0} & -\mathbf{M}^{-1}(\mathbf{q})\mathbf{C}(\mathbf{q},\mathbf{v}) \end{bmatrix} \begin{Bmatrix} \mathbf{q} \\ \mathbf{v} \end{Bmatrix} + \begin{Bmatrix} \mathbf{0} \\ \mathbf{M}(\mathbf{q})^{-1}\left[-\mathbf{G}(\mathbf{q}) + \mathbf{B}(\mathbf{q})\mathbf{u} + \mathbf{E}(\mathbf{q})\mathbf{d}\right] \end{Bmatrix} \tag{14}$$

which represents a system of first order differential equations and corresponds to the dynamics of the system under the influence of the control forces and disturbances.

2.3 Linearized Equations of Motion

To design the disturbance observer, the dynamical system in Eq. 14 is linearized to obtain a Linear Time Invariant (LTI) model, according to Eq. 15.

$$\dot{\mathbf{x}} = \mathbf{A}\mathbf{x} + \mathbf{B}_u\mathbf{u} + \mathbf{B}_d\mathbf{d}, \tag{15}$$

where the matrices $\mathbf{A}$, $\mathbf{B}_u$ and $\mathbf{B}_d$ are calculated using the first order Taylor expansion around the equilibrium point $\mathbf{q}^* = \{\mathbf{0}_{16\times1}\}^T$ with $\mathbf{u}^* = \{-(m+m_p)\,g, 0, 0, 0\}$ considering $\mathbf{d}^* = \{0,0,0,0,0,0\}^T$. The linearized matrices are:

$$\mathbf{A} = \begin{bmatrix} \mathbf{0}_{8\times8} & \mathbf{I}_{8\times8} \\ \mathbf{A}_n & \mathbf{0}_{8\times8} \end{bmatrix}$$

with

$$\mathbf{A}_n = \begin{bmatrix} 0 & 0 & 0 & 0 & -\frac{g(m+m_p)}{m} & 0 & 0 & \frac{gm_p}{m} \\ 0 & 0 & 0 & \frac{g(m+m_p)}{m} & 0 & 0 & -\frac{gm_p}{m} & 0 \\ 0 & 0 & 0 & 0 & 0 & 0 & 0 & 0 \\ 0 & 0 & 0 & 0 & 0 & 0 & 0 & 0 \\ 0 & 0 & 0 & 0 & 0 & 0 & 0 & 0 \\ 0 & 0 & 0 & 0 & 0 & 0 & 0 & 0 \\ 0 & 0 & 0 & \frac{g(m+m_p)}{ml} & 0 & 0 & -\frac{g(m+m_p)}{ml} & 0 \\ 0 & 0 & 0 & 0 & \frac{g(m+m_p)}{ml} & 0 & 0 & -\frac{g(m+m_p)}{ml} \end{bmatrix}$$

$$\mathbf{B}_u = \begin{bmatrix} \mathbf{0}_{10\times4} \\ \mathbf{B}_n \\ \mathbf{0}_{2\times4} \end{bmatrix}$$

with

$$\mathbf{B}_n = \begin{bmatrix} \frac{1}{m+m_p} & 0 & 0 & 0 \\ 0 & \frac{1}{I_{xx}} & 0 & 0 \\ 0 & 0 & \frac{1}{I_{yy}} & 0 \\ 0 & 0 & 0 & \frac{1}{I_{zz}} \end{bmatrix}$$

$$\mathbf{B}_d = \begin{bmatrix} & & & \mathbf{0}_{8\times 6} & & \\ \frac{1}{m} & 0 & 0 & 0 & 0 & 0 \\ 0 & \frac{1}{m} & 0 & 0 & 0 & 0 \\ 0 & 0 & \frac{1}{m+m_p} & 0 & 0 & \frac{1}{m+m_p} \\ 0 & 0 & 0 & 0 & 0 & 0 \\ 0 & 0 & 0 & 0 & 0 & 0 \\ 0 & 0 & 0 & 0 & 0 & 0 \\ 0 & \frac{1}{Lm} & 0 & 0 & -\frac{1}{Lm_p} & 0 \\ -\frac{1}{Lm} & 0 & 0 & \frac{1}{Lm_p} & 0 & 0 \end{bmatrix}$$

2.4 Disturbance Observer Design

In the mathematical characterization of dynamical systems, only the main contributing effects are modeled. In applications with UAVs, blade flapping, flexible structure, model uncertainties and wind gusts can be lumped as disturbances acting on the system. These perturbations are expected in a real environment and degrade performance, especially tracking performance. To deal with this disturbances, Proportional-Integral-Derivative (PID) controllers can asymptotically stabilize the system in the presence of constant disturbances by means of the "I" portion of the controller by compromising the settling time and overshoot performance given by the "P" portion; however, this type of controller is not capable of rejecting non constant disturbances (Shihua, 2014). Other methods like sliding mode control (SMC) are designed to account for the worst case scenario, which result in a compromise between performance and robustness against disturbances. In the Disturbance Observer-Based Control (DOBC), an estimate of the disturbance is calculated and feed to the controller, which is then compensated by calculating adequate inputs. The disturbance estimation error is calculated as:

$$\mathbf{e}_d = \hat{\mathbf{d}} - \mathbf{d} \tag{16}$$

With the LTI model of the UAV and payload system from Eq. 15 and assuming that the disturbance is approximately constant, i.e., $\dot{\mathbf{d}} \approx \mathbf{0}$, an auxiliary variable $\mathbf{z}$ can be defined such that the estimate of the disturbance is (Yang *et al.*, 2010):

$$\dot{\mathbf{z}} = -\mathbf{L}\mathbf{B}_d(\mathbf{z} + \mathbf{L}\mathbf{x}) - \mathbf{L}\left(\mathbf{A}\mathbf{x} + \mathbf{B}_u\mathbf{u}\right) \tag{17}$$

$$\hat{\mathbf{d}} = \mathbf{z} + \mathbf{L}\mathbf{x}, \tag{18}$$

where $\mathbf{L}$ is the observer gain matrix. The disturbance estimation error dynamics is calculated as:

$$\begin{aligned} \dot{\mathbf{e}}_d &= \dot{\hat{\mathbf{d}}} - \dot{\mathbf{d}} \\ &= \dot{\mathbf{z}} + \mathbf{L}\dot{\mathbf{x}} \\ &= -\mathbf{L}\mathbf{B}_d(\mathbf{z} + \mathbf{L}\mathbf{x}) - \mathbf{L}\left(\mathbf{A}\mathbf{x} + \mathbf{B}_u\mathbf{u}\right) + \mathbf{L}\left(\mathbf{A}\mathbf{x} + \mathbf{B}_u\mathbf{u} + \mathbf{B}_d\mathbf{d}\right) \\ &= -\mathbf{L}\mathbf{B}_d\hat{\mathbf{d}} + \mathbf{L}\mathbf{B}_d\mathbf{d} \\ &= -\mathbf{L}\mathbf{B}_d\mathbf{e}_d \end{aligned} \tag{19}$$

which is asymptotically stable if the matrix $-\mathbf{L}\mathbf{B}_d$ has eigenvalues in the Left Half Plane (LHP) in the complex plane. This type of observer requires the knowledge of the state $\mathbf{x}$, inputs $\mathbf{u}$ and the linearized system dynamic matrices $\mathbf{A}$, $\mathbf{B}_u$, $\mathbf{B}_d$. The assumption of constant disturbances is used for the observer design, but varying disturbances are also estimated.

3. CONTROLLER

The UAV and payload system is an underactuated mechanical system with 4 control inputs and 8 degrees of freedom. This result in the impossibility for the system to accelerate in an arbitrary direction in the configuration space, resulting in additional complexity to design a feasible controller (Raffo *et al.*, 2011).

The control objective is to track the desired trajectories $\mathbf{r}_d$, i.e., asymptotically stabilize the tracking error calculated as $e_i = q_{i,d} - q_i$ for $i = \{x,\ y,\ z\}$. The dynamical system is expressed in an underactuated form (Brandão *et al.*, 2013):

$$\begin{bmatrix} \mathbf{M}_{pp} & \mathbf{M}_{pa} \\ \mathbf{M}_{ap} & \mathbf{M}_{aa} \end{bmatrix} \begin{Bmatrix} \ddot{\mathbf{q}}_p \\ \ddot{\mathbf{q}}_a \end{Bmatrix} + \begin{Bmatrix} \mathbf{E}_p \\ \mathbf{E}_a \end{Bmatrix} = \begin{Bmatrix} \mathbf{0} \\ \mathbf{F} \end{Bmatrix}. \tag{20}$$

The subscripts a and p denote the active and passive degrees of freedom respectively. $\mathbf{q}_p = \{x, y, \alpha,\ \beta\}^T$ is the passive generalized coordinates, and $\mathbf{q}_a = \{z, \phi, \theta, \psi\}^T$ the active. To express the system in the form of Eq. 20, the forces acting

in the translational dynamics, i.e., the first three equations from Eq. 13, are expressed in the body frame of reference using Eq. 2:

$$\mathbf{RM}(:3,:)\ddot{\mathbf{q}} + \mathbf{RC}(:3,:)\dot{\mathbf{q}} + \mathbf{RG}(:3) = \mathbf{RB}(:3,0)\mathbf{u} + \mathbf{RE}(:3,:)\mathbf{d} \tag{21}$$

$\mathbf{M}$ is first expressed in $\mathbf{M}_{aa}$, $\mathbf{M}_{ap}$, $\mathbf{M}_{pa}$ and $\mathbf{M}_{pp}$ are the partitions of matrix $\mathbf{M}$ of Eq. 13 described in the body frame of reference. The matrices $\mathbf{E}_p$ and $\mathbf{E}_a$ correspond to the Coriollis, gravitational and disturbance forces acting in the actuated and non-actuated degrees of freedom respectively.

Applying the feedback linearization results in expressing the system as follows:

$$\mathbf{F} = \bar{\mathbf{M}}_{aa}\ddot{q}_a + \bar{\mathbf{E}}_a, \tag{22}$$

where:

$$\bar{\mathbf{M}}_{aa} = \mathbf{M}_{aa} - \mathbf{M}_{au}\mathbf{M}_{uu}^{-1}\mathbf{M}_{ua},$$

$$\bar{\mathbf{E}}_a = \mathbf{E}_a - \mathbf{M}_{au}\mathbf{M}_{uu}^{-1}\mathbf{E}_p.$$

Defining an auxiliar variable η_a for the active degrees of freedom, a control law is obtained:

$$\bar{\mathbf{M}}_{aa}\eta_a + \bar{\mathbf{E}}_a = \bar{\mathbf{M}}_{aa}\ddot{q}_a + \bar{\mathbf{E}}_a \tag{23}$$

$$\eta_a = \ddot{\mathbf{q}}_a. \tag{24}$$

$$\eta_a = \ddot{q}_a^d + \mathbf{K}_{P1}\tanh\left(\mathbf{K}_{P2}\tilde{\mathbf{q}}_a\right) + \mathbf{K}_{D1}\tanh\left(\mathbf{K}_{D2}\dot{\tilde{\mathbf{q}}}_a\right) \tag{25}$$

To control the passive degrees of freedom, the virtual inputs for the passive coordinates are calculated:

$$u_x = \frac{m\eta_x - d_x}{U_1} \tag{26}$$

$$u_y = \frac{m\eta_y - d_y}{U_1} \tag{27}$$

with η_x and η_y being the components of $\eta_p = \{\eta_x, \eta_y,\ \eta_\alpha,\ \eta_\beta\}^T$ calculated as:

$$\eta_p = \mathbf{K}_{P3}\tanh\left(\mathbf{K}_{P4}\mathbf{e}_p\right) + \mathbf{K}_{D3}\tanh\left(\mathbf{K}_{D4}\dot{\mathbf{e}}_p\right) \tag{28}$$

with $\mathbf{K}_{P3}$, $\mathbf{K}_{P4}$, $\mathbf{K}_{D3}$ and $\mathbf{K}_{D4}$ diagonal and positive definite matrices. Using this approach, the attitude reference to track the passive coordinates are obtained as:

$$\phi_d = \sin^{-1}\left(u_x s_\psi - u_y c_\psi\right) \tag{29}$$

$$\theta_d = \sin^{-1}\left(\frac{u_x c_\psi + u_y s_\psi}{c_{\phi_d}}\right) \tag{30}$$

4. RESULTS AND DISCUSSION

To simulate a realistic disturbance, the wind drag force exerted on the UAV center of mass and on payload is modeled according to Eq. 31, where $C_{d,i}$ is the drag coefficient assumed as constant, $\mathbf{v}_i$ is the relative velocity of the payload or UAV with respected to the wind, calculated as $\mathbf{v}_i = \dot{\mathbf{r}}_i + \mathbf{u}_\infty$ with $\mathbf{u}_\infty$ is the wind velocity.

$$\mathbf{d}_i = C_{d,i}|\mathbf{v}_i|\mathbf{v}_i. \tag{31}$$

The mission consist of transporting a payload by trajectory parameterized in the time $\mathbf{r}_d(t)$ and is simulated by solving numerically the system of nonlinear differential equations shown in Eq. 14 using the fifth-order Runge-Kutta algorithm with time step of $\Delta t = 2 \cdot 10^{-3}$s. Two different situations are simulated: the first is denominated as the "Reference" and correspond to the UAV subjected to the disturbance forces with a standard controller. The second situation is the "Observed" case in which the disturbances are compensated using the estimates from Eq. 18. The physical parameters from the UAV and payload used in both simulations are: $m = 2$kg, $I_{xx} = 0.04$kg·m^2, $I_{yy} = 0.04$kg·m^2, $I_{zz} = 0.03$kg·m^2, $g = 9.81$m·s^{-2}, $m_p = 0.4$kg and $l = 2$m. A constant wind field of $\mathbf{u}_\infty = \{2, 1, 0\}^T$ is assumed. The parameters used for calculating the wind drag are $C_{d,v} = 0.1875$ and $C_{d,p} = 0.0122$ for the UAV and payload respectively.

The observer gain is designed according to Eq. 17 and Eq. 18 and is show in Eq. 32. This choice of gains result in the eigenvalues $\lambda_{1,2} = -1.51 \pm 6.27j$, $\lambda_{3,4} = -6.14 \pm 9.90j$, $\lambda_5 = -7.52$ and $\lambda_6 = -4.62$.

$$\mathbf{L} = \begin{bmatrix} 0.0 & 0.0 & 0.0 & 0.0 & 0.0 & 0.0 & 0.0 & 0.0 & 15.0 & 7.0 & 3.0 & 0.0 & 0.0 & 0.0 & 3.0 & 1.0 \\ 0.0 & 0.0 & 0.0 & 0.0 & 0.0 & 0.0 & 0.0 & 0.0 & 10.0 & 15.0 & 20.0 & 0.0 & 0.0 & 0.0 & 5.0 & 2.0 \\ 0.0 & 0.0 & 0.0 & 0.0 & 0.0 & 0.0 & 0.0 & 0.0 & -7.0 & 12.0 & 10.0 & 0.0 & 0.0 & 0.0 & -2.0 & 3.0 \\ 0.0 & 0.0 & 0.0 & 0.0 & 0.0 & 0.0 & 0.0 & 0.0 & 5.0 & 3.0 & -6.0 & 0.0 & 0.0 & 0.0 & 8.0 & 10.0 \\ 0.0 & 0.0 & 0.0 & 0.0 & 0.0 & 0.0 & 0.0 & 0.0 & -6.0 & -10.0 & 3.0 & 0.0 & 0.0 & 0.0 & -10.0 & 13.0 \\ 0.0 & 0.0 & 0.0 & 0.0 & 0.0 & 0.0 & 0.0 & 0.0 & 5.0 & -20.0 & 5.0 & 0.0 & 0.0 & 0.0 & 8.0 & -2.0 \end{bmatrix} \quad (32)$$

Figure 2 shows the simulated results. It is possible to compare the desired position, indicated by the cyan and dashed lines (- -), with the simulated positions from the "Reference", indicated by (—) and the "Observed" case, represented by (—). Figure 2a shows no significant differences in the "Reference" and "Observed" simulations; however, in Fig. 2b the "Observed" case show a lower overshoot when the UAV reach the desired position. In the $\hat{k}$ direction, the disturbance observer improved the rise time.

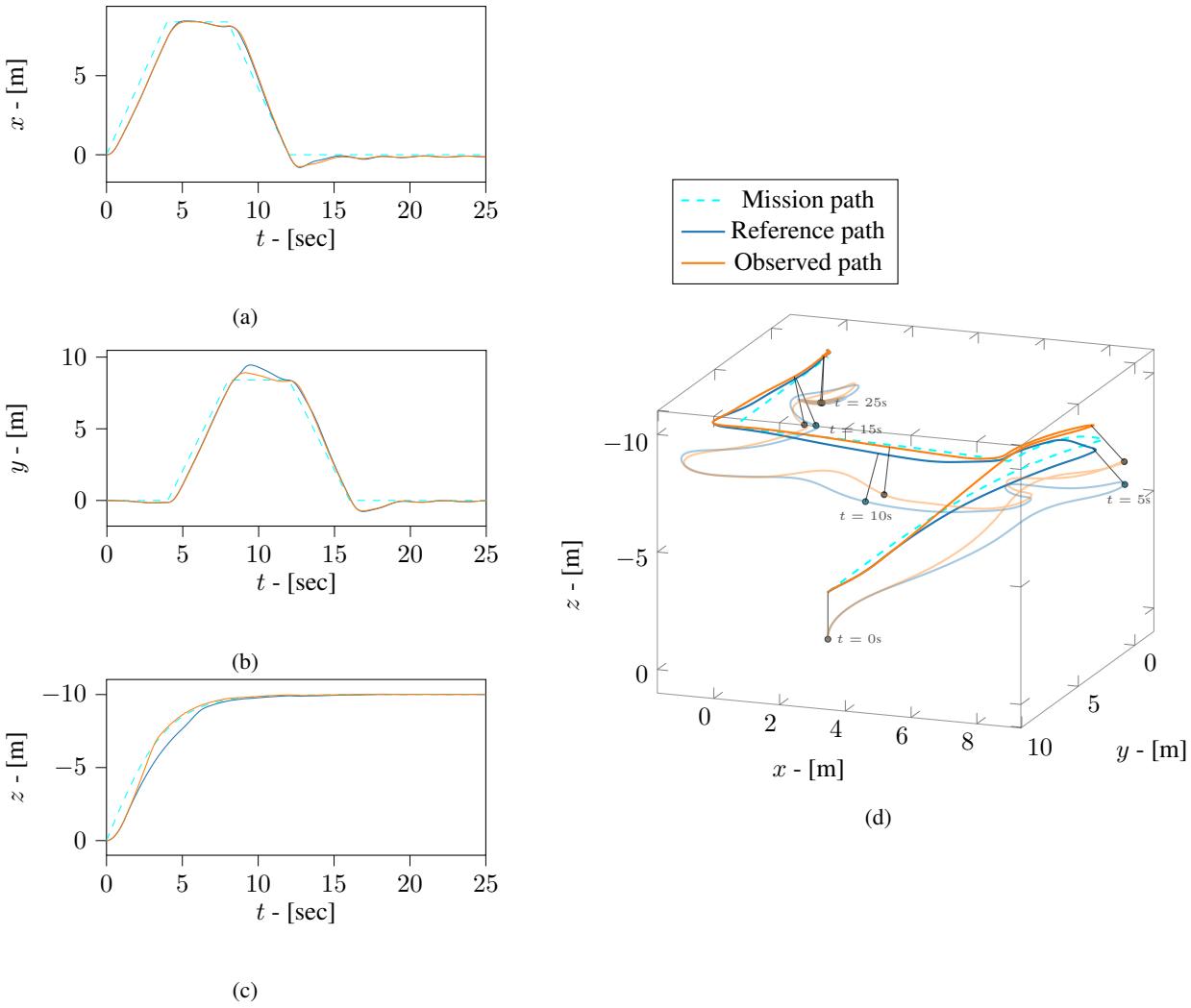

Figure 2: Simulation results for the UAV and payload system for different conditions. Position of the UAV in the x (a), y (b), z (c) directions and trajectories of the UAV and payload in (d).

The wind drag force modelled using Eq. 31 and used in the simulations is estimated with the disturbance observer, which are used in the controller to calculate the inputs according to Eq. 26 and Eq. 27. The modeled disturbances and estimated disturbances from the "Observed" case are shown in Fig. 3. According to the simulations, the disturbance observer was capable of estimating approximately the disturbances acting on the system; however besides the wind gust, it also estimates the nonlinear forces which were neglected with the assumption of a LTI system during the observer design, which explain part of the deviations from the applied external disturbances with the estimated disturbance, especially in Fig. 3e-3f.

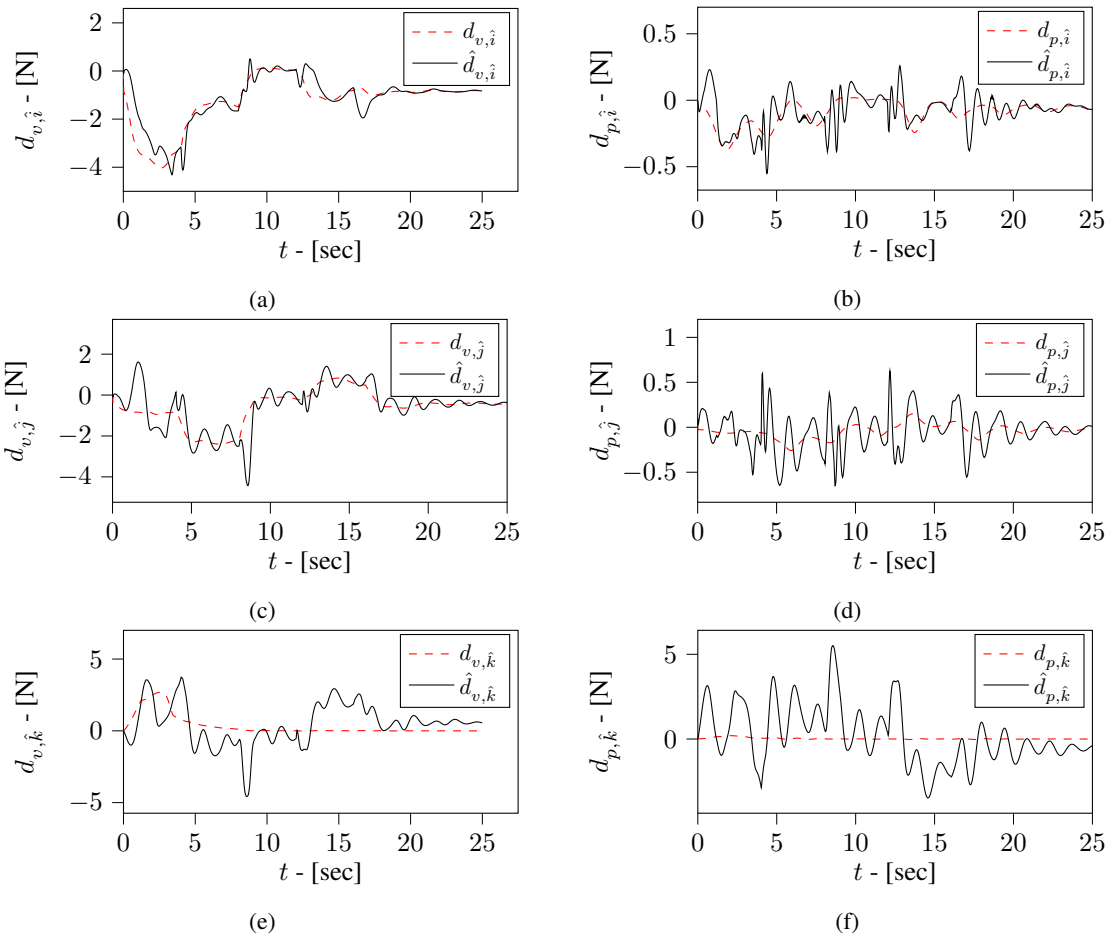

Figure 3: Disturbance applied to the UAV in the $\hat{i}$ (a), $\hat{j}$ in (c) and $\hat{k}$ in (e) directions, and to the payload in the $\hat{i}$ (b), $\hat{j}$ (d) and $\hat{k}$ (f) directions. Dashed lines represents the simulated disturbance and solid lines the estimate from the observer.

To evaluate the controller performance in tracking the desired path, three metrics are calculated (Schultz and Rideout, 1961): the IAE (integral of absolute error) in Eq. 33, the ISE (integral of square error) which penalizes larger differences in Eq. 34 and the ITAE (integral of time multiplied by absolute error) in Eq. 35 which is permissive for large initial errors but penalizes tracking error at latter instants of time. A small value for the metrics indicates a good tracking performance.

Calculating the metrics with the simulated data, as shown in Table 1, it is possible to verify that the performance from the system using the disturbance observer is slightly superior than from the reference case, presenting a reduction of 21.5% in the IAE, 10.3% for the ISE and 7.3% for the ITAE. This demonstrates that the disturbance observer improves the tracking performance for this particular system, especially in the beginning, indicated by the lower reduction of the ITAE comparing with the IAE and ISE.

$$\text{IAE} = \int_0^{t_f} \|\mathbf{e}\| dt \tag{33}$$

$$\text{ISE} = \int_0^{t_f} \mathbf{e}^T \mathbf{e} dt \tag{34}$$

$$\text{ITAE} = \int_0^{t_f} t\|\mathbf{e}\| dt \tag{35}$$

Table 1: Performance metrics calculated for the “Reference” and “Observed” cases.

Condition	IAE	ISE	ITAE
Reference	$2.0426 \cdot 10^1$	$1.8205 \cdot 10^1$	$1.4817 \cdot 10^2$
Observed	$1.6018 \cdot 10^1$	$1.6317 \cdot 10^1$	$1.3737 \cdot 10^2$

5. CONCLUSIONS

The disturbance observer using linearized dynamics is successful in estimating the disturbance forces acting on the system. By calculating control inputs that compensate the estimated disturbance force in the controller, an improvement in the system trajectory tracking performance is demonstrated with the reduction of the tracking error metrics. The strategy of estimating the disturbance have great benefits; for instance, more accurate tracking of trajectories allow the safe use of the UAV in environments with large number of obstacles, such as in indoor flight, dense forests or in flight formations. For future work, the application of DOBC strategy will be extended by estimating higher order disturbances and also using the nonlinear plant to obtain more accurate estimates.

6. ACKNOWLEDGEMENTS

The authors would like to thanks the São Paulo State University for the opportunity to and the GMSINT group. The second author gives special thanks to the National Council for Scientific and Technological Development (CNPq) Grant no. 429963/2016-5 for the financial support.

7. REFERENCES

Brandão, A.S., Filho, M.S. and Carelli, R., 2013. "High-level underactuated nonlinear control for rotorcraft machines". In *2013 IEEE International Conference on Mechatronics (ICM)*. pp. 279–285. doi:10.1109/ICMECH.2013.6518549.

Chen, C.Y. and Cheng, M.Y., 2012. "Adaptive disturbance compensation and load torque estimation for speed control of a servomechanism". *International Journal of Machine Tools and Manufacture*, Vol. 59, pp. 6–15. doi:10.1016/j.ijmachtools.2012.03.006. URL https://doi.org/10.1016/j.ijmachtools.2012.03.006.

Chen, W.H., Yang, J., Guo, L. and Li, S., 2016. "Disturbance-observer-based control and related methods—an overview". *IEEE Transactions on Industrial Electronics*, Vol. 63, No. 2, pp. 1083–1095. doi:10.1109/TIE.2015.2478397.

Niu, D., Zhu, Y., Chen, X., Li, Q., Wang, X., Yang, Y. and Wang, S., 2020. "An anti-sway positioning control method via load generalized position tracking with disturbance observer". *Measurement and Control*, Vol. 53, No. 9-10, pp. 2101–2110. doi:10.1177/0020294020962133. URL https://doi.org/10.1177/0020294020962133.

Raffo, G.V., Ortega, M.G. and Rubio, F.R., 2011. "Path tracking of a UAV via an underactuated control strategy". *European Journal of Control*, Vol. 17, No. 2, pp. 194–213. doi:10.3166/ejc.17.194-213. URL https://doi.org/10.3166/ejc.17.194-213.

Sariyildiz, E., Oboe, R. and Ohnishi, K., 2020. "Disturbance observer-based robust control and its applications: 35th anniversary overview". *IEEE Transactions on Industrial Electronics*, Vol. 67, No. 3, pp. 2042–2053. doi:10.1109/TIE.2019.2903752.

Schultz, W.C. and Rideout, V.C., 1961. "Control system performance measures: Past, present, and future". *IRE Transactions on Automatic Control*, Vol. AC-6, No. 1, pp. 22–35. doi:10.1109/TAC.1961.6429306.

Shihua, 2014. *Disturbance observer-based control : methods and applications*. CRC Press, Taylor & Francis Group, Boca Raton, FL. ISBN 9781466515802.

Xie, L.L. and Guo, L., 2000. "How much uncertainty can be dealt with by feedback?" *IEEE Transactions on Automatic Control*, Vol. 45, No. 12, pp. 2203–2217. doi:10.1109/9.895559.

Yang, J., Li, S. and Chen, W.H., 2010. "Autopilot design of bank-to-turn missiles using state-space disturbance observers". In *UKACC International Conference on CONTROL 2010*. Institution of Engineering and Technology. doi:10.1049/ic.2010.0454. URL https://doi.org/10.1049/ic.2010.0454.

8. RESPONSIBILITY NOTICE

The authors are solely responsible for the printed material included in this paper.